ORIGINAL ARTICLE

Time-of-flight PET/CT using low-activity protocols: potential implications for cancer therapy monitoring

Iain Murray · Antonis Kalemis · Joe Glennon ·
Syed Hasan · Shuaib Quraishi · Thomas Beyer ·
Norbert Avril

Abstract

Introduction Accurate quantification of tumour tracer up-take is essential for therapy monitoring by sequential PET imaging. In this study we investigated to what extent a reduction in administered activity, synonymous with an overall reduction in repeated patient exposure, compromised the accuracy of quantitative measures using time-of-flight PET/CT.

Methods We evaluated the effect of reducing the emission count statistics, using a 64-channel GEMINI TF PET/CT system. Experiments were performed with the NEMA IEC body phantom at target-to-background ratios of 4:1 and 10:1. Emission data for 10 s, 30 s, 1 min, 2 min, 5 min and 30 min were acquired. Volumes of interest fitted to the CT outline of the spheres were used to calculate recovery coefficients for each target-to-background ratio and for different reconstruction algorithms. Whole-body time-of-flight PET/CT was performed in 20 patients 62±4 min after injection of 350±40 MBq (range 269–411 MBq) ^{18}F-FDG. From the acquired 2 min per bed position list mode data, simulated 1-min, 30-s and 15-s PET acquisitions were created. PET images were reconstructed using the TOF-OSEM algorithm and analysed for differences in SUV measurements resulting from the use of lower administered activity as simulated by reduced count statistics.

Results In the phantom studies, overall we identified no significant quantitation bias over a wide range of acquired counts. With acquisition times as short as 10 s, lesions as small as 1 cm in diameter could still be identified. In the patient studies, visual analysis showed that emission scans as short as 15 s per bed position sufficiently identified tumour lesions for quantification. As the acquisition time per bed position decreased, the differences in SUV quantification of tumour lesions increased relative to the 2-min reference protocol. However, SUVs remained within the limits of reproducibility required for therapy monitoring. Measurements of SUVmean within the region of interest were less prone to noise than SUVmax, and with the 30-s per bed position 95% confidence limits were ±11% or ±0.7 SUV.

Conclusion Short time acquisitions, synonymous with reduced injected activity, performed on a TOF-based PET/CT system are feasible without encountering significant bias. This could translate into clinical protocols using lower administered activities particularly for serial PET studies.

I. Murray · S. Hasan · S. Quraishi · N. Avril (✉)
Department of Nuclear Medicine,
Barts and The London School of Medicine,
West Smithfield (QE II),
London EC1A 7BE, UK
e-mail: n.e.avril@qmul.ac.uk

A. Kalemis · J. Glennon
Philips Healthcare,
The Observatory, Castlefield Road,
Reigate RH2 0FY, UK

T. Beyer
cmi-experts,
Pestalozzistr.3,
Zurich 8032, Switzerland

Introduction

Positron emission tomography (PET) provides rapid, reproducible, noninvasive in vivo assessment and quantifi-

cation of several biological processes targeted by anticancer therapies [1]. PET with ^{18}F-fluorodeoxyglucose (FDG) reflects tissue glucose metabolism and reveals important diagnostic information in a variety of tumours [2]. FDG PET allows the prediction of response early in the course of therapy as well as determining the viability of residual masses after completion of treatment [1]. The diagnostic accuracy of PET is further increased by coregistered CT, as in combined PET/CT systems [3].

Accurate quantification of tracer uptake in tumour tissue is essential for therapy monitoring particularly for early prediction of response using sequential PET studies [4, 5]. Standardized uptake values (SUV) are frequently used to provide a semiquantitative measure of tissue tracer accumulation by normalizing the tissue radioactivity concentration measured with PET to injected activity and body weight. This allows comparison between PET studies performed in the same patient at different times. Previous studies have demonstrated that SUVs provide reproducible parameters of tumour glucose utilization [1, 6]. The differences between repeated measurements were approximately normally distributed and changes of more than 20% were outside the 95% range for spontaneous fluctuations and could therefore be considered to reflect therapy-induced changes.

PET treatment monitoring studies necessarily involve a number of PET acquisitions prior to and over the course of therapy. Therefore, the radiation exposure needs to be taken into consideration. However, it has been shown that the increased noise levels associated with lower count statistic acquisitions can result in an increased bias in SUV measurements of up to 15%, particularly when using SUVmax [7].

Time-of-flight (TOF) PET has recently been introduced into the design of clinical whole-body PET/CT [8]. A precise measurement is made of the difference in arrival times between a pair of coincident photons, thus narrowing the probability distribution of the location of the annihilation event along the line-of-response (LOR). Compared to conventional PET, TOF PET improves the signal-to-noise ratio [9]. This is especially true in large patients or with low count statistics [10, 11]. Furthermore, the additional TOF information enables reconstruction to converge faster than with a non-TOF algorithm [12].

The aim of this study was to investigate whether a reduction in administered activity would compromise the accuracy of quantitative measures using TOF PET/CT. We assumed that lower activity concentrations can be simulated with shorter scan times. Our hypothesis was that we would maintain the accuracy of measurements of radioactivity concentration as acquisition times were reduced. Therefore, we analysed both phantom and clinical data derived from a Philips GEMINI TF system to explore the potential bias in

quantitation with low count statistics. Furthermore, the clinical data were used to investigate and quantify any deterioration in SUV reproducibility at reduced count statistics.

Materials and methods

Phantom studies

A NEMA IEC body phantom (Data Spectrum Corporation) with sphere diameters of 10, 13, 17, 22, 28 and 37 mm was filled with a total activity of 50 MBq ^{18}F-FDG, such that the concentration of the background compartment was 5 kBq/ml and the target-to-background activity ratio (TBR) of the spheres was 4:1. The background compartment activity of 5 kBq/ml was typical of the activity concentration observed in the normal liver tissue of patients.

All data were acquired on a 64-channel GEMINI TF PET/CT system (Philips Healthcare, Cleveland, OH). Imaging was initiated with a planar scout scan used to define the axial range of the study followed by a volumetric CT acquisition. CT parameters were 120 kVp, 50 mAs, and 5 mm slice width and separation. In order to simulate the effect of lowering the activity in the phantom, six consecutive PET acquisitions were made over the same target volume (single bed position) with scan times of 10 s, 30 s, 1 min, 2 min, 5 min and 30 min, respectively. The same CT acquisition was used for attenuation correction in all cases. This experiment was repeated twice to provide an estimate of error in the measured uptake. All acquisitions were performed such that the bed position was centred on the plane of the spheres. Subsequently, three repeat experiments were carried out with the phantom filled to a TBR of 10:1 using the same imaging parameters to investigate scanner performance at higher signal-to-noise levels.

Image reconstruction and analysis

Images were reconstructed using both an ordered subsets expectation maximization algorithm incorporating TOF information (TOF-OSEM) [13], and a row action maximum likelihood algorithm (3D-RAMLA) [14], both supplied as routine software by the manufacturer of the PET/CT system. The reconstruction parameters for TOF-OSEM were three iterations and 33 subsets, and for 3D-RAMLA two iterations. These are the default reconstruction parameters recommended by the manufacturer.

Phantom images were analysed using volumes of interest (VOIs) defined to match the CT outlines of the phantom spheres. For every image reconstruction, both

the mean and maximum activity concentrations were recorded for each sphere. The background VOI was limited axially by an extent defined by the largest sphere in order to ensure that axial variations in noise did not influence the analysis.

Measured TBRs were calculated by dividing either the maximum or mean VOI activity concentration by the mean activity concentration measured across a background VOI. Recovery coefficients were then calculated by dividing the measured TBR by the known TBR at which the phantom was filled. Hence, for each phantom acquisition at TBR of 4:1 and 10:1, recovery coefficients were measured as a function of both time per bed position and sphere diameter. In order to test objectively for bias with low count statistics a paired t-test was carried out to compare the TBRs quantified with a 30-min acquisition with 5-min, 2-min, 1-min, 30-s and 10-s acquisitions, respectively. Comparisons were made for each reconstruction at the TBRs of 10:1 and 4:1, and p-values less than 0.05 were considered significant.

A TBR-based analysis may lead to a potential bias in the background quantification obscuring changes in the sphere measurements. We therefore also analysed directly the activity concentrations measured in the background VOIs. To objectively test the hypothesis that there was no relationship between the acquisition time and the activity quantified (i.e. no bias) we carried out a linear regression of the data. The deviation of the fitted slope from zero was tested through a significance test of the correlation observed (R^2).

Clinical PET/CT imaging

Imaging protocol

The PET/CT acquisition data from 20 consecutive patients were used. The analysis was part of an audit, which was registered and approved by our review board. Patients fasted for 6 h prior to FDG PET/CT imaging and their blood glucose level was measured prior to injection of FDG (4.7±0.7 mmol/l, range 4.0–7.0 mmol/l). Patients received 350±40 MBq (range 269–411 MBq) of ^{18}F-FDG intravenously. Following tracer injection, patients rested in a comfortable reclined position for 55 min. PET/CT imaging was initiated with a planar scout scan to define the axial range of the study followed by a volumetric CT acquisition. CT parameters were 120 kVp, 50 mAs, and 5 mm slice width and separation. Scanning was performed from the base of the skull down to the mid-thighs. PET acquisition was initiated at 62±4 min (range 57–70 min) after FDG injection using a 2 min per bed position protocol. The bed overlap for clinical studies was 50%.

Image reconstruction and analysis

The 2 min per bed position list mode emission data file was resampled to simulate PET emission scans based upon 1-min, 30-s and 15-s bed positions. Images were reconstructed using the TOF OSEM. Furthermore, a total of 59 foci of increased FDG uptake larger than 2 cm, classified as tumour deposits by clinical analysis, were identified in 20 patients. Qualitative evaluation was performed by an experienced observer for all 59 foci to assess the visualization of lesions at different count statistics. The level of FDG uptake was analysed using standardized 15-mm diameter ROIs placed in the plane of the highest tumour activity. For each patient the same ROI was applied to the same location on the 2-min, 1-min, 30-s and 10-s images. In all cases both the maximum and mean SUV (SUVmax and SUVmean) were recorded. Bland-Altman plots were created to assess whether uptake measurements on the lower count statistic images were able to reproduce the corresponding reference measurements. The distributions of the differences between uptake measurements were checked for normality using the D'Agostino-Pearson test [15]. In addition, correlation plots of the corresponding measurements in the lower count statistics and reference images were created and Spearman's correlation coefficient was calculated as a secondary measure of reproducibility of the SUV values.

Results

Phantom studies

Transaxial images of the NEMA IEC phantom for TBRs of 4:1 and 10:1 and TOF OSEM reconstruction as well as 3D-RAMLA algorithm over the entire range of PET acquisition times are shown in Fig. 1. As the acquisition time decreased from 30 min to 10 s, there was a corresponding increase in noise and a decrease in image contrast on visual image inspection. The loss of contrast resolution was more pronounced at a TBR of 4:1, where the smallest sphere (1 cm) were not seen with the 30-s and 10-s acquisition times. However, at a TBR of 10:1 all spheres were visualized including with the 10-s acquisition time.

The analysis of the background activity quantification showed no bias (Fig. 2). No statistically significant difference was observed in the measurement of background activity over the entire range of acquisition times ($p>0.05$) for either reconstruction algorithm. An additional important result was that there was no significant systematic error (bias) in the semiquantitative measurements of radioactive uptake and contrast using the TOF-OSEM algorithm. Figure 3 shows the recovery coeffi-
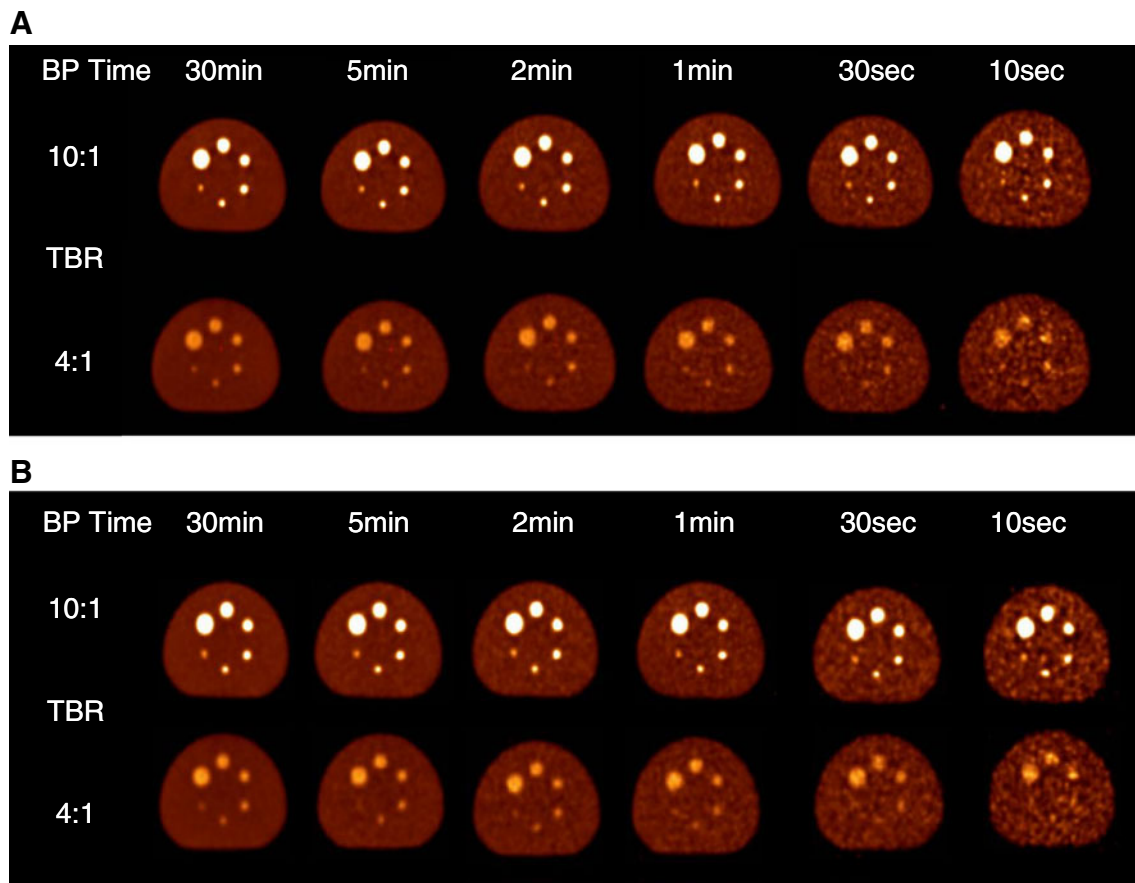
Fig. 1 Transaxial images of the NEMA IEC phantom spanning the middle of the sphere compartments for all acquisition times and both TBRs considered, for (**a**) the TF-OSEM and (**b**) the 3D-RAMLA (*BP Time* acquisition time per bed position)

cients based upon the mean activity concentration in the VOI. These are shown for each TBR and reconstruction algorithm as a function of both acquisition time and sphere size. In the more clinically relevant TBR of 4:1, the variation in quantitative measures increased as the sphere size and acquisition time decreased. There were no statistically significant differences for the mean values between the 30-min PET data acquisition used as the reference and lower count-statistic measurements for both the 10:1 TBR and the 4:1 TBR.

For phantom images reconstructed with 3D-RAMLA, larger differences between the 30-min reference data and lower count statistics datasets were observed and found to be significant ($p=0.02$, 0.002, 0.007, 0.03 for 30 min vs. 5 min, 30 min vs. 2 min, 30 min vs. 1 min, and 30 min vs. 30 s, respectively). In the 10:1 TBR acquisitions the signal to background levels were higher and the consistency of quantitative measures was even more clearly demonstrated (Fig. 3). Comparing the two reconstruction algorithms, a difference in recovery coefficients was noted for sphere sizes of less than 22 mm at 4:1 TBR, independent of the acquisition time. However, this was not found for the 10:1 TBR.

The SUVmax is frequently used in the clinical setting to measure the level of FDG uptake in tumour lesions. Therefore, we calculated recovery coefficients for the 4:1
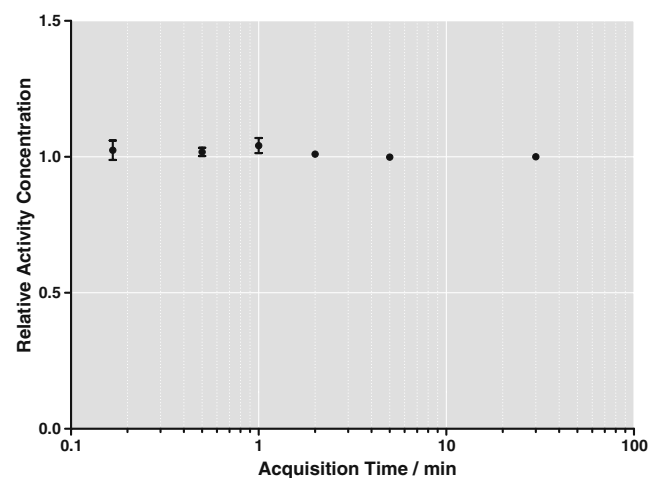

Fig. 2 Activity concentrations measured in background VOIs as a function of acquisition time. The analysis is based on a NEMA IEC phantom at a 10:1 TBR with activity concentrations shown relative to the 30-min values (means±SD). No bias in the activity quantitation is apparent
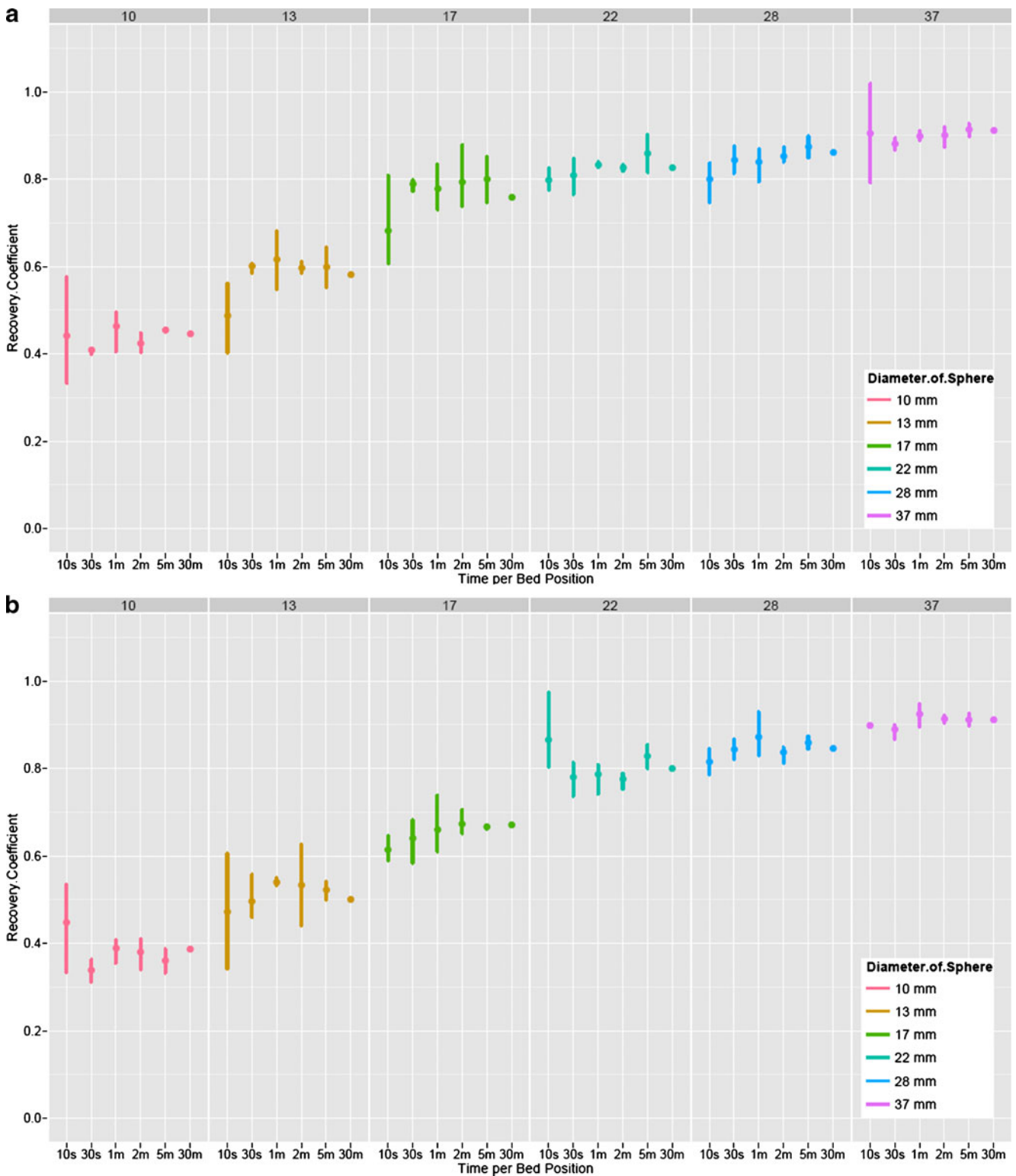
Fig. 3 Recovery coefficients (SUVmean) as a function of sphere size and acquisition time per bed position for (**a**) 4:1 TBR for TF-OSEM, (**b**) 4:1 TBR for 3D-RAMLA, (**c**) 10:1 TBR for TF-OSEM, and (**d**) 10:1 TBR for 3D-RAMLA

TBR TOF-OSEM dataset using the maximum activity within the VOI (Fig. 4). The results show that as acquisition time decreases there is a systematic error introduced in the observed quantitative measures ($p < 0.05$). SUVmax was generally higher across all sphere sizes and particularly for the largest spheres. With the lowest acquisition time of 10 s per bed position a bias of about 25% was observed for the 37-mm sphere.
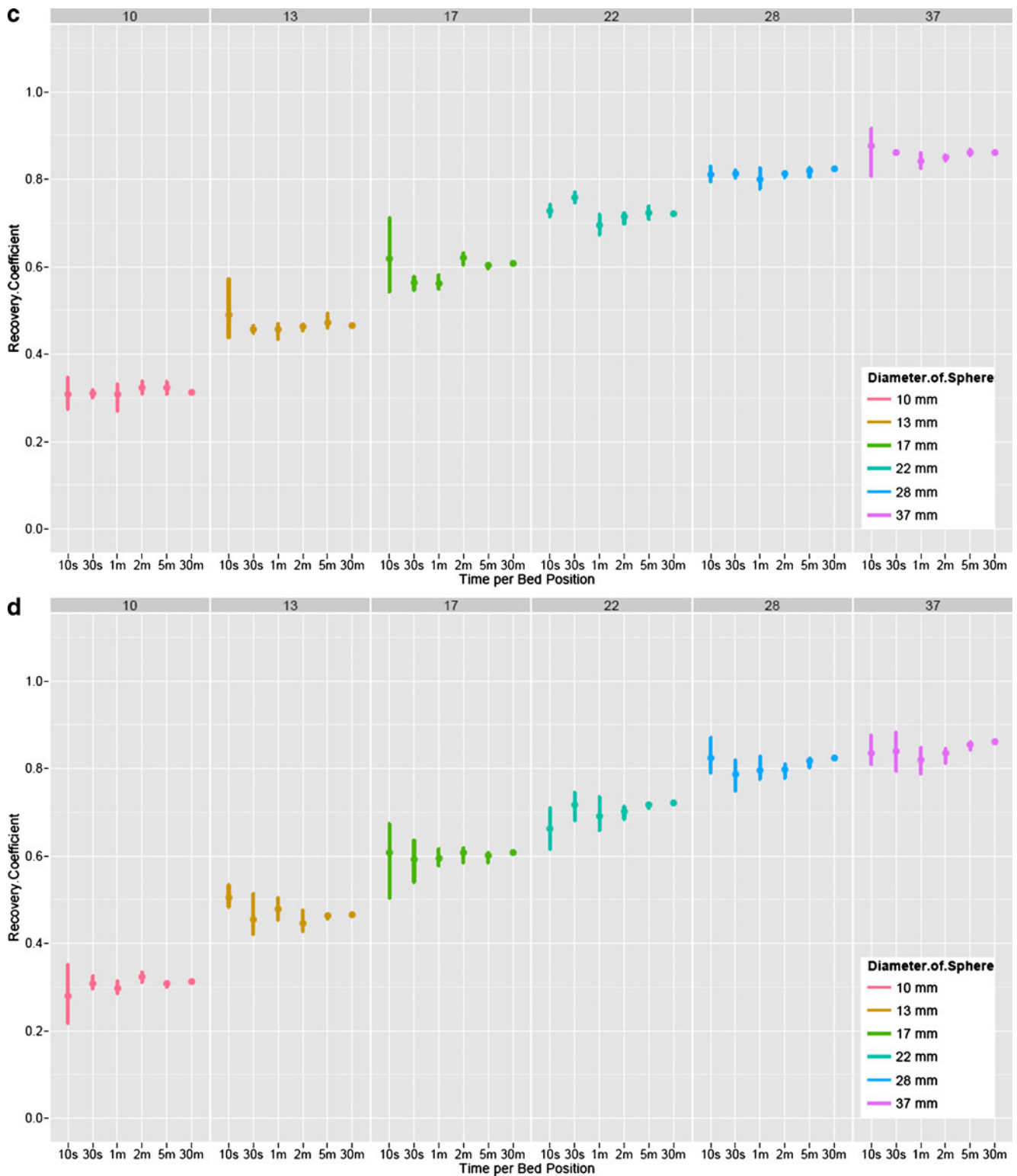
Fig. 3 (continued)

Patient studies

An example of the image quality achieved with reduced count statistics is shown in Fig. 5. For all patient PET images, lesions identified on the diagnostic 2 min acquisition per bed position were identifiable throughout the whole set of lower count reconstructions, even with 15 s per bed position.
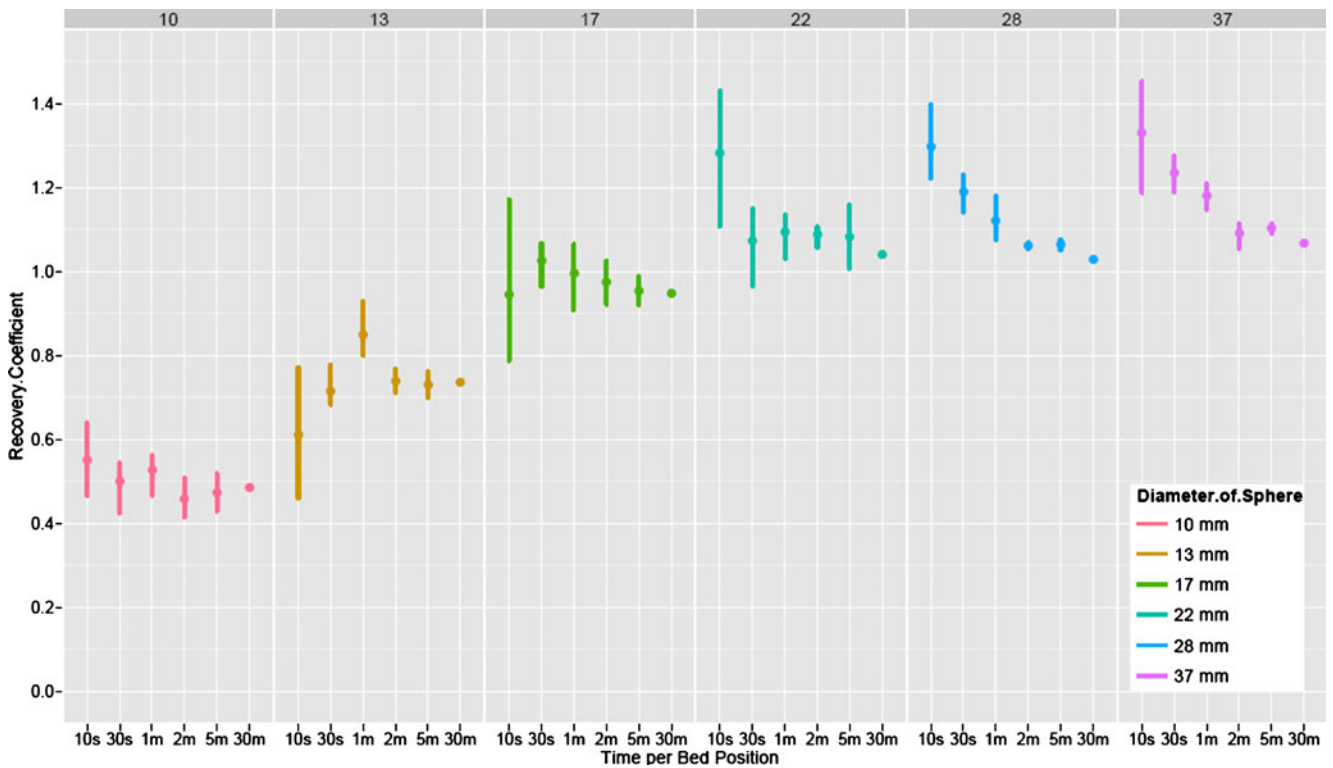
Fig. 4 Recovery coefficients calculated using SUVmax as a function of sphere size and time per bed position for 4:1 TBR for TF-OSEM. The effects of noise are clearly shown as increases in both variance and bias

For the quantitative analysis, the 2 min acquisition per bed position dataset was used as the reference against which to compare lower count statistic datasets. The Bland-Altman plots created to illustrate the differences between reference and low count statistic measurements of SUVmean showed no bias as a function of SUV (Fig. 6). The 95% confidence intervals expressed as both absolute and percentage differences in SUV are listed in Table 1. The Bland-Altman plots and the associated confidence intervals showed that reproducibility deteriorated as acquisition time decreased. SUVmean was more reproducible than SUVmax in the context of decreasing count statistics. However, a systematic bias as noted with measurements based upon maximum activity in the

Fig. 5 Clinical PET image performance achieved with various acquisition times. A 43-year-old female (68 kg) with breast cancer imaged 1 h after injection of 350 MBq ^{18}F-FDG imaged at 2 min, 1 min, 30 s and 15 s per bed position
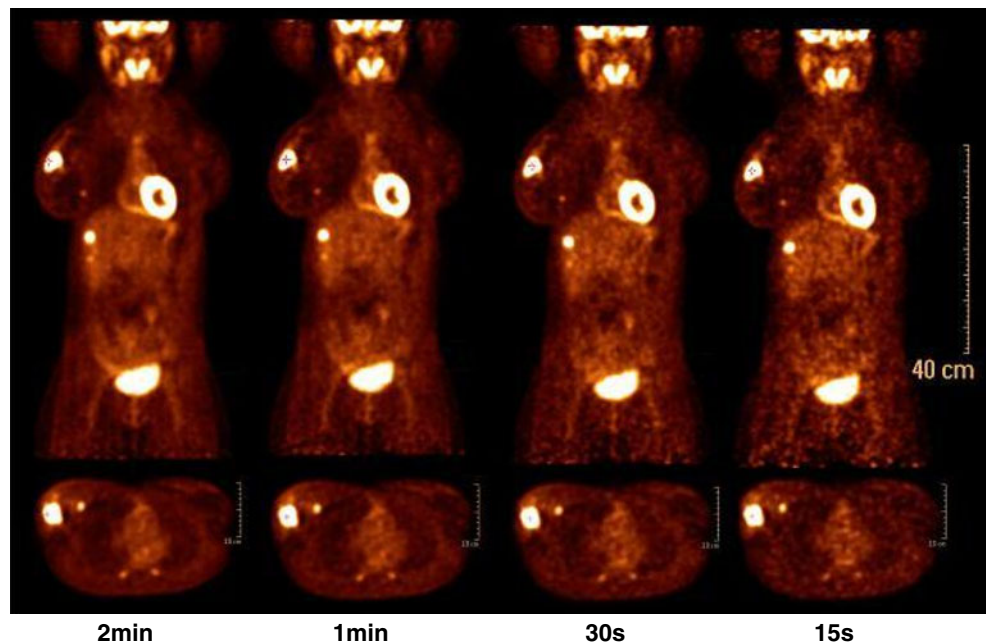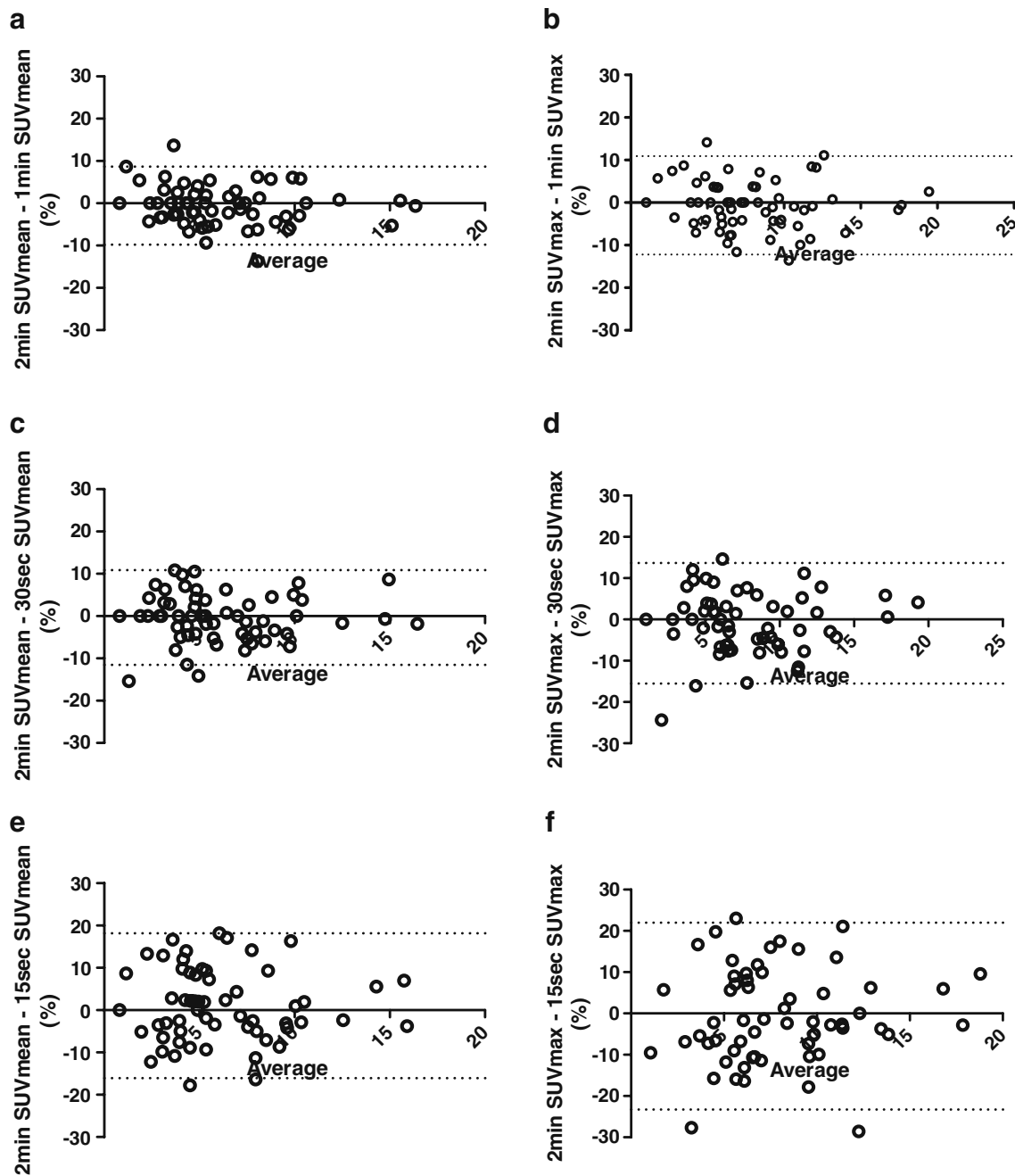
Fig. 6 Bland-Altman plots of SUVmean (**a**, **c**, **e**) and SUVmax (**b**, **d**, **f**) showing differences between 2 min and 1 min (**a**, **b**), 2 min and 30 s (**c**, **d**) and 2 min and 15 s (**e**, **f**)

phantom studies was not observed in the clinical measurements of SUVmax.

As shown in Fig. 7, there were high correlations between the reference 2-min PET data acquisition per bed position, and the 1 min, 30 s and 15 s per bed position acquisitions for both SUVmean and SUVmax measurements. Spearman's correlation coefficient (r) confirmed these observations as for all graphs r was 0.99 or more ($r^2 \geq 0.98$) apart from the 2 min vs. 15 s SUVmax for which it was 0.95 ($r^2 = 0.90$).

Discussion

We demonstrated that low-count PET acquisitions as simulated by short acquisition times are feasible with TOF PET/CT technology without significant bias. The emission acquisition times were as short as 15 s per bed position in patient studies and 10 s in phantom studies, thereby simulating typical clinical activity concentrations. This represents a substantial improvement over previous PET technology with acquisition times typically of

Table 1 95% confidence intervals of the absolute and percentage differences in SUVs of malignant foci observed with reduced count statistics

	2min vs. 1min	2min vs. 30s	2min vs. 15s
SUVmean			
Absolute	−0.67 to 0.56	−0.72 to 0.72	−1.0 to 1.2
Percentage	−9.8 to 8.8	−11.5 to 11.5	−16.2 to 18.7
SUVmax			
Absolute	−1.0 to 0.9	−1.1 to 1.1	−1.6 to 1.7
Percentage	−12.2 to 11.2	−15.2 to 14.3	−22.2 to 21.9

several minutes per bed position. As expected, a decrease in acquisition time resulted in noisier images which in turn led to a corresponding decrease in image contrast (Fig. 1).

It is well known that the OSEM reconstruction algorithm applied to low-count statistic acquisitions may lead to non-Poisson statistics in the image [16]. However, in our study acquisition times as short as 30 s per bed position produced interpretable PET images from phantom studies performed with clinically applicable radioactivity concentrations and TBRs. Furthermore, we were able to obtain accurate measurements of radioactivity concentrations with 30 s per bed position consistent with those measured with 2-min acquisition time as reference (Fig. 6). A previous study has found a bias dependent on the count statistic of up to 75% with 10 s per bed position using a dedicated brain PET scanner [17]. The most likely explanation for the lack of bias observed in our study is that the GEMINI TF scanner utilizes a list-mode version of OSEM in order to incorporate TOF information [18] with precorrected list-mode

Fig. 7 Correlation plots of SUVmean (**a**, **c**, **e**) and SUVmax (**b**, **d**, **f**) between the reference 2 min per bed position vs. 1 min, 30 s and 15 s per bed position
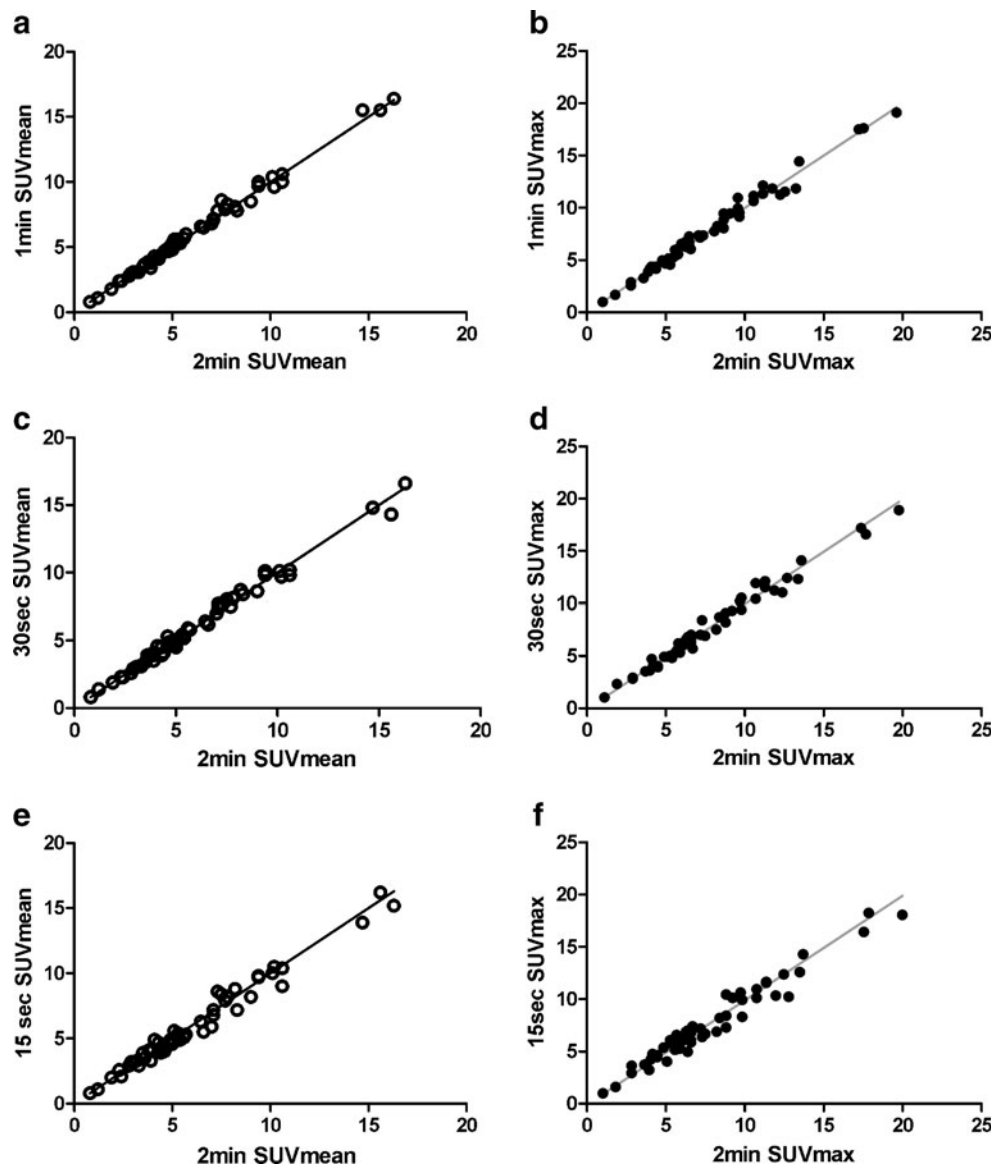
events for detector normalization, isotope decay, system dead-time and crystal timing. Attenuation, scatter and randoms are corrected in the reconstruction system matrix rather than in the LOR space. Previous work has shown that algorithms that are required by design to implement nonnegativity constraints in image space rather than in sinograms/LORs are less prone to bias [19].

It should be noted that the findings discussed above relate to the mean activity concentration measured within a VOI. However, the use of the maximum activity within a VOI resulted in radioactivity concentration measurements more affected by low count statistics ($p<0.05$). From the phantom data, the activity concentration based upon a single voxel was more readily affected by increased noise than the mean radioactivity concentration within a VOI (Fig. 4). Nevertheless, the increased noise with low count statistics could potentially be addressed by optimization of PET image reconstruction parameters or with the use of smoothing filters, and needs to be further explored.

The principal advantage of TOF PET is that the noise in an image is decreased by a factor proportional to the square root of $2D/c\Delta t$, where D is the object diameter, c is the speed of light and Δt is the time resolution of the system [9]. Hence, this may be a reason that the reproducibility of SUVmean in particular remained relatively robust as the statistics were reduced. In Fig. 3 a difference in contrast performance is apparent between the TOF-OSEM data and the 3D-RAMLA algorithms for the smaller phantom spheres at a TBR of 4:1. PET contrast recovery curves are primarily related to the spatial resolution of the tomograph. Although TOF information does not improve spatial resolution, in comparison to other non-TOF algorithms the TOF-OSEM requires fewer iterations to reach convergence [8].

Our second aim was to establish the reproducibility of clinical SUV measurements between a reference baseline PET dataset acquired at 2 min per bed position and shorter acquisition times as a surrogate for lower injected activities. Previous studies, which assessed the reproducibility of FDG uptake measurements (SUV) in malignant tumours between two identical image acquisitions found 95% confidence limits varying from ±0.5 to ±0.9 for SUVmean and up to ±2.0 for SUVmax [20–22]. We demonstrated that lowering the count statistics to the equivalent of a 30-s PET data acquisition per bed position led to reproducibilities of ±0.7 SUV for SUVmean and ±1.1 SUV for SUVmax with biases of −0.3% and −0.9%, respectively.

Although reducing count statistics had an observable effect on reproducibility this should be considered in the context of the typical level of change observed during treatment regimens. While no definitive level of change has been agreed, a decrease of more than 20–25% in tumour FDG uptake is recognized as a reasonable definition of metabolic response during treatment [6]. While there are other technical factors [23] (e.g. ROI

definition technique) that should be taken into consideration when assessing the reliability of SUV measurements, the present analysis demonstrated that the additional uncertainty due to lower count statistics (injected activity) could fall sufficiently below this threshold.

How can these findings be translated into new clinical protocols? The baseline FDG PET/CT scan prior to therapy and the end-of-treatment scan should be acquired at best diagnostic image quality. However, FDG-PET/CT imaging during therapy, e.g. after the first or second cycle of chemotherapy, could potentially be performed with lower injected activities. It is important that the acquisition times per bed position remain consistent throughout sequential PET/CT imaging to ensure that the PET data for each part of the body are acquired at the same time relative to tracer injection. Hence the application of our findings would be towards lower activity protocols rather than faster scan times. For example, in the UK activities for FDG PET/CT generally range up to 400 MBq ^{18}F-FDG. If FDG PET/CT imaging during therapy could be accomplished with 100–150 MBq ^{18}F-FDG, this would reduce the radiation exposure from approximately 8 mSv to 2–3 mSv per scan in a standard adult. Reduced activities for treatment monitoring would particularly facilitate the more frequent use of FDG PET/CT in clinical trials of therapeutic agents and potentially the use of multi-PET tracer protocols for noninvasive tumour characterization by assessing multiple biological parameters in the same patient. Other applications might include breath-hold imaging of lung lesions as demonstrated by Torizuka et al. [24].

Certain limitations of our study need to be considered. We simulated lower activity imaging by clipping the list-mode files to produce images based upon shorter acquisition times. Therefore, we were unable to identify any potential benefits from imaging at lower activities such as a reduced rate of random coincidences. Conversely, the use of short acquisition time scans as a surrogate for low activities may also mask any artefacts or errors in quantitation that could be introduced through patient motion over the normal period of acquisition.

Our phantom studies compared a non-TOF algorithm (3D-RAMLA) with TOF-OSEM reconstructions. Unfortunately, it was not possible with the PET/CT system used to reconstruct emission data from multiple bed position acquisitions with 3D-RAMLA. Therefore, a head-to-head comparison of quantitation of clinical images reconstructed with a non-TOF reconstruction could not be made.

Conclusion

We demonstrated that short time acquisitions, synonymous with reduced injected activity, performed on a TOF-based PET/CT system resulted in images that, although susceptible to higher levels of noise, provided meaningful quantitative

results without significant bias. Our findings could have positive implications for the design of clinical trials aiming to perform serial PET/CT imaging over the course of treatment.

References

1. Weber WA. Positron emission tomography as an imaging biomarker. J Clin Oncol 2006;24(20):3282–92.
2. Fletcher JW, Djulbegovic B, Soares HP, et al. Recommendations on the use of 18F-FDG PET in oncology. J Nucl Med 2008;49 (3):480–508.
3. Czernin J, Allen-Auerbach M, Schelbert HR. Improvements in cancer staging with PET/CT: literature-based evidence as of September 2006. J Nucl Med 2007;48:78S–88.
4. Avril NE, Weber WA. Monitoring response to treatment in patients utilizing PET. Radiol Clin North Am 2005;43(1):189–204.
5. Stahl A, Ott K, Schwaiger M, Weber WA. Comparison of different SUV-based methods for monitoring cytotoxic therapy with FDG PET. Eur J Nucl Med Mol Imaging. 2004;31(11):1471–8.
6. Weber WA, Figlin R. Monitoring cancer treatment with PET/CT: does it make a difference? J Nucl Med 2007;48 Suppl 1:36S–44.
7. Boellaard R. Standards for PET image acquisition and quantitative data analysis. J Nucl Med 2009;50(Suppl 1):11S–20.
8. Karp JS, Surti S, Daube-Witherspoon ME, Muehllehner G. Benefit of time-of-flight in PET: experimental and clinical results. J Nucl Med 2008;49(3):462–70.
9. Budinger TF. Time-of-flight positron emission tomography: status relative to conventional PET. J Nucl Med 1983;24(1):73–8.
10. Surti S, Karp JS, Popescu LM, Daube-Witherspoon ME, Werner M. Investigation of time-of-flight benefit for fully 3-D PET. IEEE Trans Med Imaging 2006;25(5):529–38.
11. Surti S, Karp JS. Experimental evaluation of a simple lesion detection task with time-of-flight PET. Phys Med Biol 2009;54 (2):373–84.
12. Surti S, Kuhn A, Werner ME, Perkins AE, Kolthammer J, Karp JS. Performance of Philips Gemini TF PET/CT scanner with special consideration for its time-of-flight imaging capabilities. J Nucl Med 2007;48(3):471–80.
13. Popescu LM, Matej S, Lewitt RM. Iterative image reconstruction using geometrically ordered subsets with list-mode data. IEEE Nucl Sci Symp Conf Rec 2004;1–7:3536–40.
14. Daube-Witherspoon ME, Matej S, Karp JS, Lewitt RM. Application of the row action maximum likelihood algorithm with spherical basis functions to clinical PET imaging. IEEE Trans Nucl Sci 2001;48(1):24–30.
15. D'Agostino RB, Belanger A, D'Agostino RB Jr. A suggestion for using powerful and informative tests of normality. American Statistician 1990;44(4):316–21.
16. Hoffman EJ, Huang SC, Phelps ME, Kuhl DE. Quantitation in positron emission computed tomography: 4. Effect of accidental coincidences. J Comput Assist Tomogr 1981;5(3):391–400.
17. van Velden FH, Kloet RW, van Berckel BN, Lammertsma AA, Boellaard R. Accuracy of 3-dimensional reconstruction algorithms for the high-resolution research tomograph. J Nucl Med 2009;50 (1):72–80.
18. Wang W, Hu Z, Gualtieri EE, et al. Systematic and distributed time-of-flight list mode PET reconstruction. Paper presented at: Nuclear Science Symposium Conference Record, 2006. IEEE, 2006.
19. Rahmim A, Lenox M, Reader AJ, et al. Statistical list-mode image reconstruction for the high resolution research tomograph. Phys Med Biol 2004;49(18):4239–58.
20. Weber WA, Ziegler SI, Thodtmann R, Hanauske AR, Schwaiger M. Reproducibility of metabolic measurements in malignant tumors using FDG PET. J Nucl Med 1999;40(11):1771–7.
21. Krak NC, Boellaard R, Hoekstra OS, Twisk JW, Hoekstra CJ, Lammertsma AA. Effects of ROI definition and reconstruction method on quantitative outcome and applicability in a response monitoring trial. Eur J Nucl Med Mol Imaging 2005;32(3):294–301.
22. Nahmias C, Wahl LM. Reproducibility of standardized uptake value measurements determined by 18F-FDG PET in malignant tumors. J Nucl Med 2008;49(11):1804–8.
23. Boellaard R, Krak NC, Hoekstra OS, Lammertsma AA. Effects of noise, image resolution, and ROI definition on the accuracy of standard uptake values: a simulation study. J Nucl Med 2004;45 (9):1519–27.
24. Torizuka T, Tanizaki Y, Kanno T, et al. Single 20-second acquisition of deep-inspiration breath-hold PET/CT: clinical feasibility for lung cancer. J Nucl Med 2009;50(10):1579–84.